metals

MDPI

Review

Factors Affecting the Mechanical Performance of High Manganese Austenitic Steel

Lei Xia [1,2,*], Ling Yan [2,*], Hongmei Zhang [1], Yan Li [2], Zhengyi Jiang [1] and Guanglong Li [2]

[1] School of Material and Metallurgy, University of Science and Technology Liaoning, Anshan 114051, China
[2] The State Key Laboratory of Metal Material for Marine Equipment and Application, Anshan Iron and Steel Research Institute of AnGang Group, Anshan 114009, China
* Correspondence: xialei0627@163.com (L.X.); yanling_1101@126.com (L.Y.); Tel.: +86-0412-5929551 (L.X.)

Abstract: High manganese austenitic steel has attracted increasing attention for its application in liquefied natural gas storage tank materials due to its excellent ductility and low cost. This paper presents an overview of the research progress of high manganese austenitic steel in recent years. As a structural material used at a low temperature environment, high manganese steel should not only have certain strength, but also good toughness to prevent brittle fracture at a low temperature. In this work, factors affecting mechanical properties of high manganese steel are discussed, possible reasons for the deterioration of low-temperature properties are analyzed, and the strengthening and toughening mechanisms of materials are elaborated, which may be beneficial to improve properties of high manganese austenitic steel.

Keywords: high manganese austenitic steel; strength; ductility; deterioration; strengthening mechanism

check for updates

Citation: Xia, L.; Yan, L.; Zhang, H.; Li, Y.; Jiang, Z.; Li, G. Factors Affecting the Mechanical Performance of High Manganese Austenitic Steel. *Metals* **2022**, *12*, 1405. https://doi.org/10.3390/met12091405

Academic Editor: Damien Fabrègue

Received: 3 August 2022
Accepted: 23 August 2022
Published: 25 August 2022

Publisher's Note: MDPI stays neutral with regard to jurisdictional claims in published maps and institutional affiliations.

Copyright: © 2022 by the authors. Licensee MDPI, Basel, Switzerland. This article is an open access article distributed under the terms and conditions of the Creative Commons Attribution (CC BY) license (https://creativecommons.org/licenses/by/4.0/).

1. Introduction

The research on liquefied natural gas storage tank materials has become increasingly active with the increasing demand of liquefied natural gas storage and transportation. At present, liquefied natural gas storage tank materials are mainly nickel series steels and invar alloy, which is expensive [1–3]. High manganese steel generally refers to alloy steels containing more than 10 wt.% manganese, which has been recognized as having an excellent ductility–strength balance [4,5]. In recent years, researchers have developed high manganese austenitic steel to replace 9Ni steel, invar alloy, and other expensive metal materials to reduce the cost and expand the application range of liquefied natural gas storage tank materials [6–9].

The materials for liquefied natural gas storage tanks are mainly used below −162 °C, and the cryogenic performance requirement of them is stringent. Inhibition of the brittle fracture at cryogenic temperatures is a key factor to improve the cryogenic performance of high manganese steel. The main reasons for the deterioration of cryogenic properties are martensite transformation during low-temperature deformation [10–12], "slipping-off" fracture caused by dislocation accumulation at grain boundaries [13,14], the influence of hydrogen embrittlement [15,16], and the segregation of impurity elements at grain boundaries, etc. [17].

The microstructure of high manganese austenitic steel is austenite at room temperature, and it has a high ductility at low temperatures. Low-carbon high manganese steel with over 30% manganese has a good impact property at low temperatures and almost no ductile–brittle transition [18]. However, the yield strength of it is relatively low due to the face-centered cubic structure [19,20]. Generally, the mechanical properties of high manganese austenitic steel are improved by alloying [6–8], grain refinement [19,21,22], and controlling the forming process, such as temperature, strain, and strain rate [23]. The deformation mechanism includes transformation-induced plasticity (TRIP) [24], twinning-induced plasticity (TWIP) [10,20], shear-induced plasticity (SIP) [25], and micro-band-induced plasticity

(MBIP) [26], etc. The high strength can be maintained, and the work hardening ability of materials can be improved to obtain good plasticity through these mechanisms.

This paper aims at focusing on the existing knowledge and research gap in high manganese austenitic steel for liquefied natural gas storage tanks. An exclusive review section on the factors affecting the mechanical properties, reasons for the deterioration of low-temperature properties, the strength, and the plastic strengthening mechanism of high manganese austenitic steel developed by different researchers is presented in this review paper as well. The structure of this review is given in Figure 1.

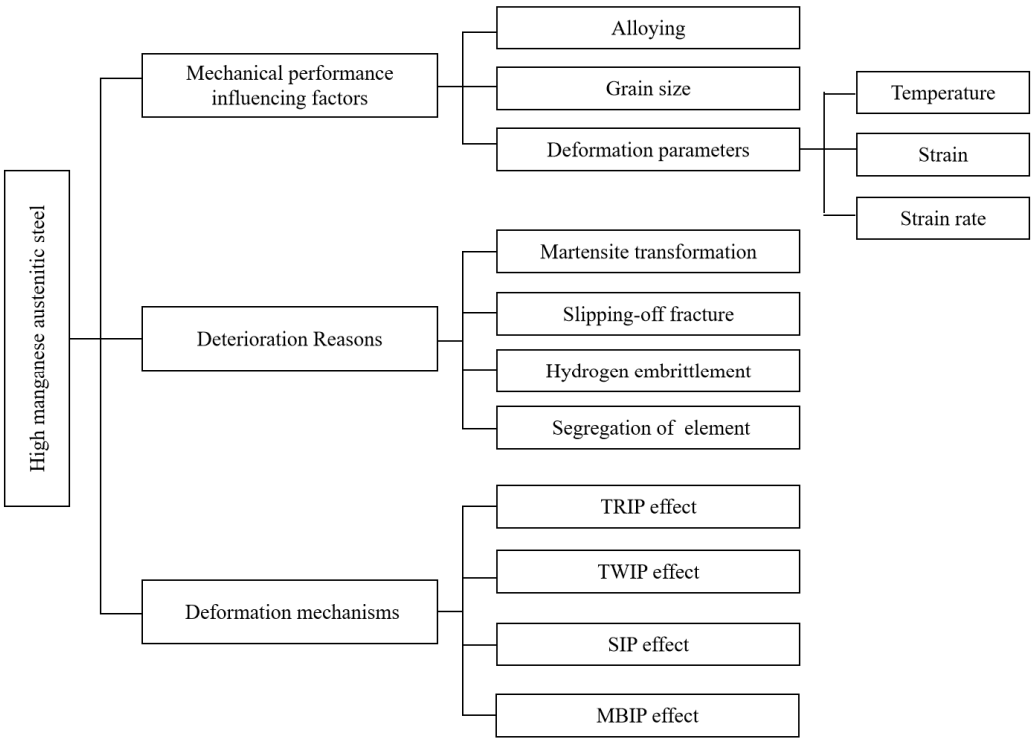

Figure 1. Structure of the current review.

2. Factors Affecting Mechanical Properties

2.1. Alloying

Increasing manganese in steels can enlarge the austenite phase zone and stabilize the austenite structure. The high manganese steel with a single-phase austenite structure can be obtained at room temperature when the manganese content exceeds a certain proportion. The single-phase austenite was obtained when the content of manganese and carbon met the Equation (1) [27].

$$\text{wt.\%Mn} + 13\text{wt.\%C} > 17 \quad (1)$$

The increase of manganese content can change the stacking fault energy (SFE) of materials. When the manganese content is lower than a certain value, the stacking fault energy of high manganese steel decreases with the increase of manganese content. The stacking fault energy of high manganese steel increases with the increase of manganese content when the manganese content is higher than a certain value (Figure 2a) [28]. Therefore, the stacking fault energy of high manganese steel can be adjusted, the deformation mode of materials can be changed, and the performance of high manganese steel can be improved by controlling the manganese content. An increasing manganese content in high manganese steels is beneficial to the occurrence of dynamic recrystallization. It will ascend the maximum flow stress of steel at low temperatures, while it leads to a smaller maximum flow stress of steel under temperatures above 700 °C [29]. A low manganese content will lead to the formation of α' martensite and affect the formability of steel, while

the formation of the brittle phase will be promoted when the manganese content is higher than 30–35% [30,31].

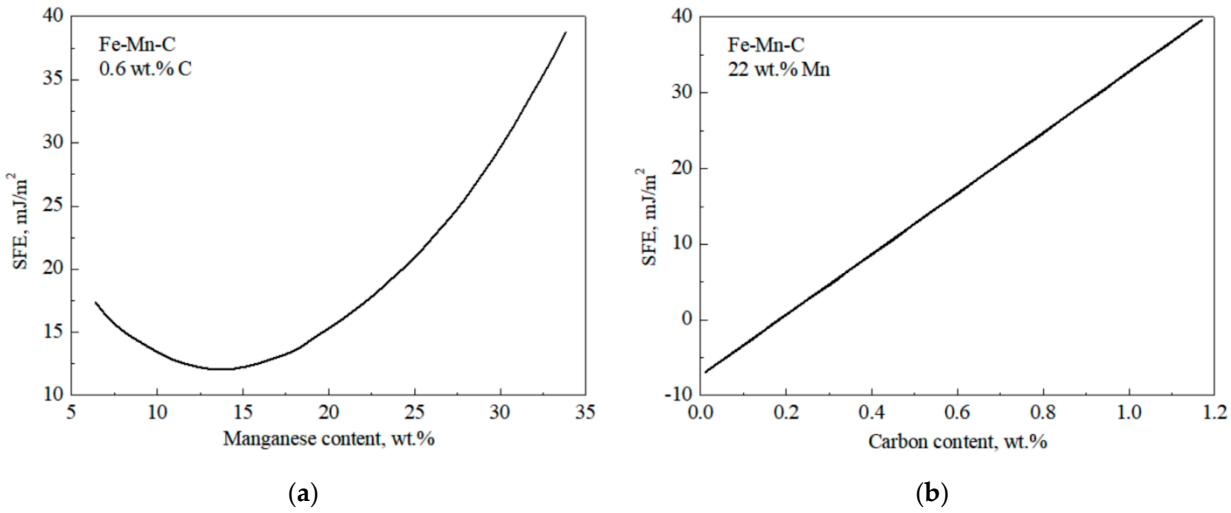

Figure 2. (**a**) Isocarbon (0.6 wt.%) and (**b**) isomanganese (22 wt.%) stacking fault energy diagrams (Reprinted with permission from Ref. [28], Copyright 2022 Springer Nature).

Carbon is also an element that can expand the austenite phase region and stabilize the austenite phase. Meanwhile, carbon atoms, which are solid–solution elements in the austenite phase, can play the role of solid–solution strengthening and improve the properties of high manganese steel. Lee [32] and Ghasri-Khouzani [33] et al. found out that the addition of carbon in Fe–Mn austenitic steels was beneficial to both the strength and ductility of steels. They were improved with increased carbon concentration. However, Koyama [34] reported that the effect of carbon content on the ductility of steel was not only related to carbon concentration, but also to strain rate. The elongation of steels increased with an increased carbon concentration at a strain rate of 10^{-2} s^{-1}, while it decreased at a strain rate of 10^{-5} s^{-1} in the Fe–Mn–C steels with 0.6 wt.% to 1.1 wt.% carbon [34]. In Fe–Mn–C alloys, the stacking fault energy increases with the increase of carbon content (Figure 2b) [28]. The stacking fault energy is not the only factor that determines the deformation mode of materials. The carbon content has an important influence on the deformation mode of high manganese steel [33,35,36]. The deformation products are mechanical ε martensite in the carbon-free steel [33,35], mechanical twins are observed for the steels with 0.2 wt.% to 0.6 wt.% carbon, and both mechanical twins and ε martensite were found in the steel with 0.06 wt.% carbon [36]. The effect of carbon on the flow behavior of high manganese steel is mainly at temperatures below 700 °C. The maximum flow stress of steel can be raised by increasing the carbon content. The influence will be weaker with the increase of temperature [29]. In high manganese austenitic steel, the yield strength (YS) is related to the content of manganese and carbon, which can be expressed by Equation (2) [37]

$$\text{YS (MPa)} = 228 + 187\text{wt.\%C} - 2\text{wt.\%Mn} \quad (2)$$

Aluminum is an element that can close the austenite phase region and infinitely expand the ferrite phase region. A single-phase ferrite is formed at room temperature when the content of aluminum exceeds a certain proportion. In addition, the increase of aluminum content not only increases the stacking fault energy of materials, but also promotes the plane dislocation slip in Fe–Mn–Al–Si alloys [38,39]. However, intermetallic compound (Fe_3Al) will precipitate when the aluminum content is too high, which will lead to brittle fracture of the material [40]. Charles [41], Chen [42], Han [43], and Takaki [44] et al. reported that the increase of aluminum also inhibited the γ austenite to ε martensite phase transformation,

which is beneficial to the formation of deformation twins. A stress-induced martensitic transformation is found in the high manganese steel without aluminum, while there are no martensites and deformation twins formed in the high manganese steel containing aluminum. Therefore, adding aluminum in high manganese steel can improve its yield strength and get a higher Charpy impact energy [7]. However, the addition of aluminum in high manganese steel will lower the strain hardening rate and tensile strength at subzero temperatures. It has little effect on the static crystallization rate of steel, but it obviously delays the occurrence of dynamic recrystallization [45]. Aluminum can also improve its corrosion resistance by forming an Al_2O_3 protective layer on the metal surface [46].

The increase of the silicon content in steel will not only close the austenite phase region, but also reduce the stacking fault energy of alloys. The alloy is more prone to martensite transformation during deformation [47]. The hydrogen embrittlement of high manganese steel in terms of both crack initiation and propagation can be obviously inhibited by adding copper in steel. The addition of copper in high manganese steel only affects the hydrogen embrittlement rate rather than the mechanism of hydrogen embrittlement (Table 1) [48]. The main role of niobium in high manganese steel is to inhibit recovery and recrystallization, especially for a large niobium addition. The solution strengthening, grain refinement, and precipitation hardening effect of niobium is limited. Niobium alloying in high manganese steel can effectively inhibit dynamic strain aging and deteriorate the cryogenic impact toughness and tensile toughness of steel (Figure 3) [49]. The yield strength of the high manganese steel can be improved with alloying chromium /nitrogen while maintaining its superior low-temperature toughness [6]. The improved strength is caused by solid–solution strengthening resulting from dissolved nitrogen and grain-boundary and precipitation strengthening resulting from the precipitation of aluminum nitride, and the former is the most effective strength mechanism [6].

Table 1. The area fraction of the intergranular-fractured region depending on the applied strain for the hydrogencharged 0Cu and 2Cu steels (Reprinted with permission from Ref. [48] Copyright 2022 Elsevier).

Engineer Strain	0Cu Steel (%)	2Cu Steel (%)
0.05	0.02	0.03
0.10	0.45	0.15
0.20	1.31	0.79
0.30	2.11	1.11

From the above analysis, it can be concluded that the effect of alloying on mechanical properties of high manganese steel varies with alloying elements. Carbon, aluminum, and nitrogen elements can be appropriately added to high manganese steel to improve its strength. Both increasing the content of aluminum and decreasing the content of niobium in steel are beneficial to the toughness.

The composition of high manganese steel can also affect the deformation parameters. An appropriate rolling and solid solution treatment temperature should be selected to avoid carbide precipitation in the process of producing high manganese steel alloyed by other elements to obtain good low-temperature toughness. Therefore, thermodynamic assessments of equilibrium phase diagrams for steel should be carried out. Wang et al. [6,50] researched phase diagrams of 22Mn, 24Mn-3.3Cr, 24Mn-3.4Cr, and 24Mn-6.3Cr-0.2N steels, as shown in Figure 4. The results showed that M_7C_3 precipitation temperatures of 22Mn, 24Mn-3.3Cr, and 24Mn-3.4Cr steels were 700 °C, 850 °C, and 860 °C, respectively. There was no $M_{23}C_6$ in the 22Mn steel, while they might be formed in 24Mn-3.3Cr, 24Mn-3.4Cr, and 24Mn-6.3Cr-0.2N steels when the temperature decreases to 710 °C, 740 °C, and 900 °C, respectively, or below. The rolling and solid solution treatment temperature of high manganese steel varies with the composition according to above results. It is better to set them above the critical precipitation temperatures to avoid carbide precipitation. The critical

precipitation temperatures rise with increased chromium content, and the rolling and solid solution treatment temperature should be set higher.

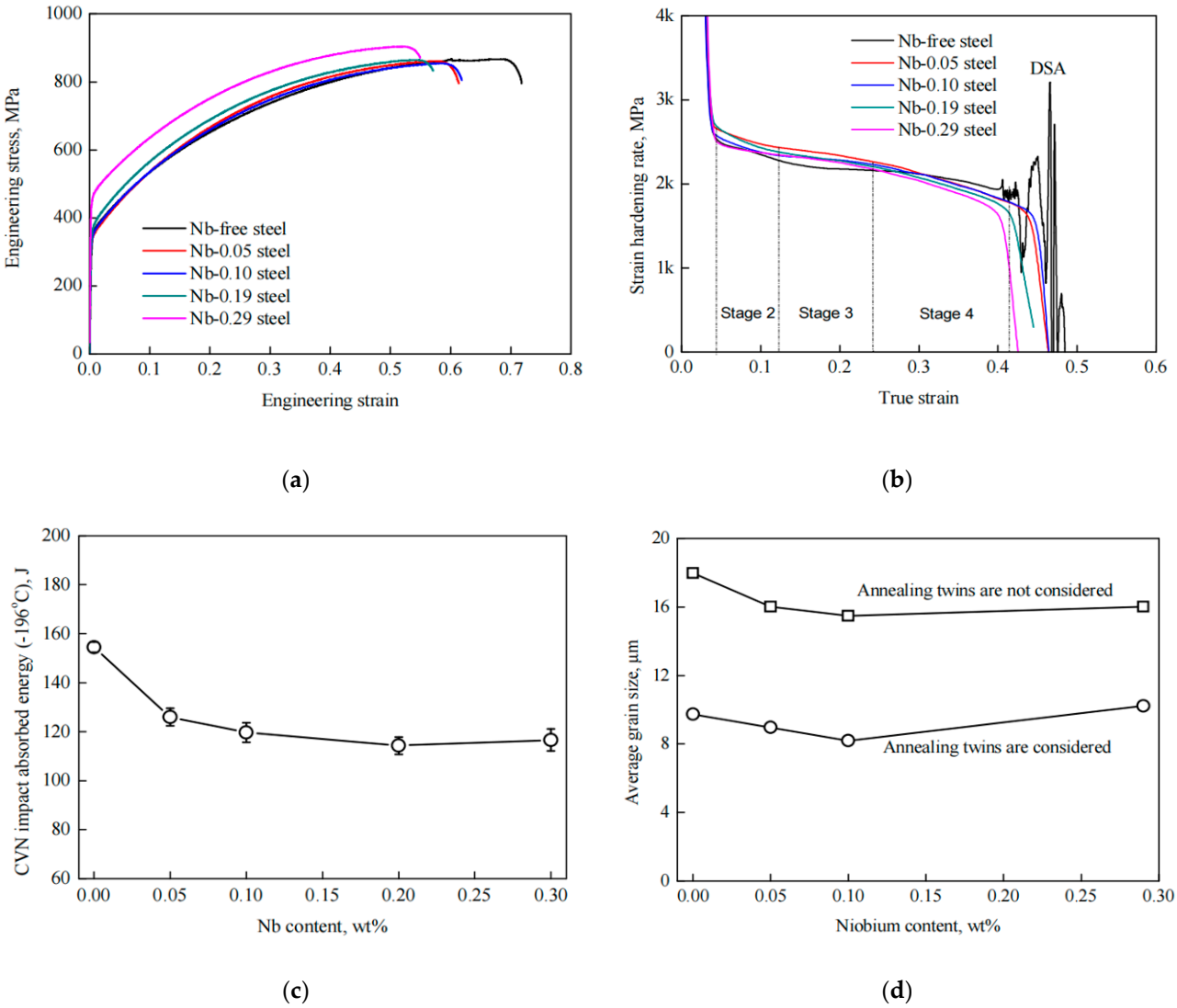

Figure 3. Effects of niobium contents on (**a**) engineering stress–strain curves, (**b**) corresponding strain-hardening curves, (**c**) Charpy V-notch impact absorbed energies at −196 °C, and (**d**) grain sizes of high manganese steel (Reprinted with permission from Ref. [49] Copyright 2022 Elsevier).

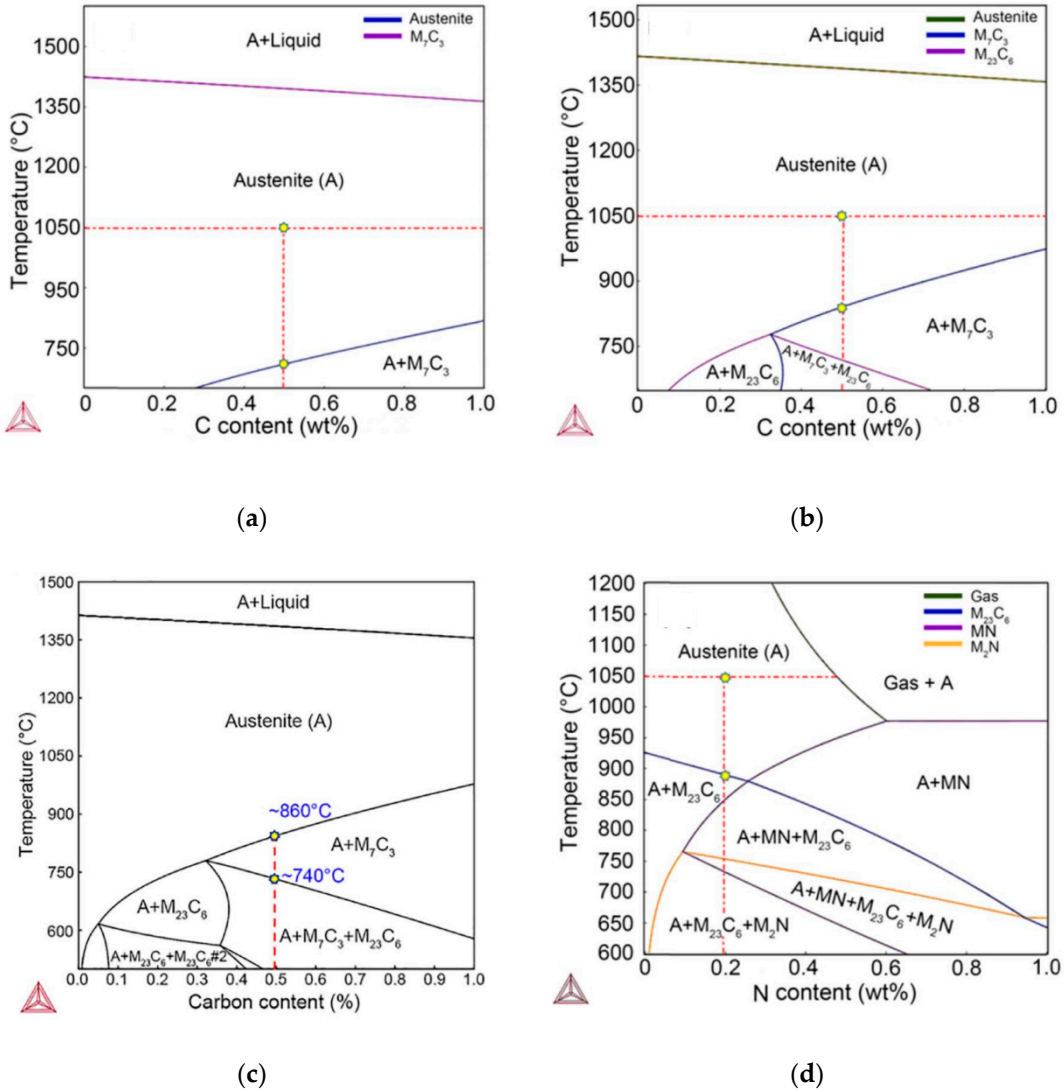

Figure 4. Phase equilibrium diagram of (**a**) 22Mn (Reprinted with permission from Ref. [6] Copyright 2022 Elsevier), (**b**) 24Mn-3.3Cr [6], (**c**) 24Mn-3.4Cr (Reprinted with permission from Ref. [50] Copyright 2022 Elsever), and (**d**) 24Mn-6.3Cr-0.2 N [6] steels.

2.2. Grain Size

Grain size has an important influence on the microstructure and properties of iron and steel. Grain refinement can improve the strength of high manganese austenitic steel without affecting its low temperature plasticity and toughness [19,21,22,51]. Generally, a finer grain size gives a larger grain boundary area and a larger proportion of grain boundary in the microstructure, and it leads to a greater strengthening effect. This phenomenon is called grain refinement, which is juxtaposed with deformation strengthening, solution strengthening, and second phase strengthening as several strengthening methods of materials. The effect of grain size on strength can be described by the Hall–Petch Equation (3) [52].

$$\sigma(\varepsilon) = \sigma_0(\varepsilon) + K(\varepsilon)d^{\frac{1}{2}} \tag{3}$$

where $\sigma(\varepsilon)$ is the yield strength of materials at a constant strain ε; σ_0 is the lattice friction force, which refers to the yield stress of undeformed single crystal when sliding; d is the grain size; and $K(\varepsilon)$ is the Hall–Petch strengthening coefficient at the strain ε.

In a constant grain size, a larger $K(\varepsilon)$ gives a greater strength increment, which proves that the effect of fine grain strengthening on the material is greater. The Hall–Petch

Equation is applicable to most materials. However, there will be an obvious "anti-Hall–Petch relationship" when the grain size decreases to nano-scale [53]. The strength will increase with the increased grain size at nano-scale [54]. However, it is difficult for the grain size of steel to reach nanometer scale due to the limitation of rolling technology. The minimum size of mass-produced high-manganese austenitic steel is more than 2 μm. Therefore, the Hall–Petch Equation can be used to express the influence of grain size on the strength of high-manganese austenitic steel [55].

Dini et al. [21] annealed Fe–31Mn–3Al–3Si steel at 850 °C for different times to obtain fine and coarse grain structures with different grain sizes, and then, they carried out a tensile test to study the effect of grain size on tensile properties of steel (Table 2). Ueji et al. [22] prepared an ultrafine-grained structure by cold-rolling and annealing, and they studied the tensile properties and twinning behavior of ultrafine-grained, fine-grained, and coarse-grained steels at room temperature (Figure 5). The results showed that the yield strength and tensile strength increased, and the plasticity decreased with the decrease of grain size. The generation of mechanical twins was restrained with the grain refinement. The yield strength of Fe–22Mn–0.6C TWIP steel can reach 700 MPa when the grain size is about 1 μm [19]. The effect of grain refinement on the mechanical performance is related to the application temperature. Wang et al. [51] researched the effect of grain size on the mechanical properties of high manganese austenitic steel at 25 °C and −196 °C and found that the effect of grain refinement on the yield strength of steel at −196 °C was stronger than that at 25 °C. The toughness and ductility of steel were improved with the increase of grain size at 25 °C. However, there was little influence at −196 °C, owing to the emergence of the micro-twin.

Table 2. Tensile properties of Fe–31Mn–3Al–3Si steel with different grain sizes (Reprinted with permission from Ref. [21] Copyright 2022 Elsevier).

Grain Size (μm)	Yield Strength (MPa)	Ultimate Tensile Strength (MPa)	Yield Strength /Ultimate Tensile Strength	Ultimate Elongation (%)
2.1	572.0	825.0	0.69	39.8
4.7	404.4	723.8	0.56	56.5
11.4	311.9	648.1	0.48	63.1
23.7	208.6	575.4	0.36	70.0
72.6	123.1	519.4	0.24	76.3

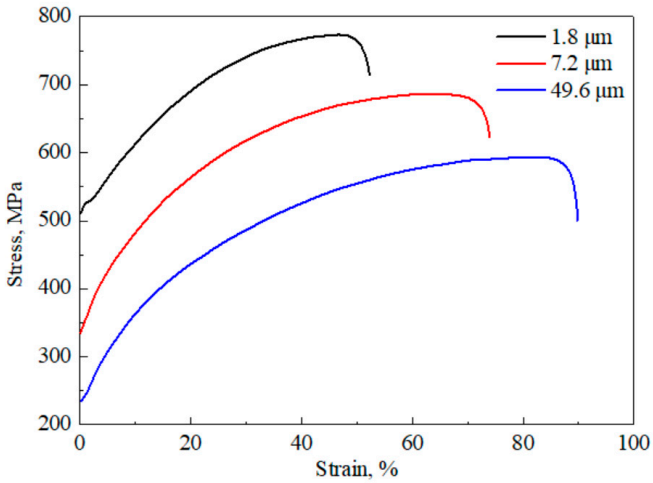

Figure 5. Stress–strain curves of the Fe–31Mn–3Al–3Si steels with different grain sizes (Reprinted with permission from Ref. [22], Copyright 2022 Elsevier).

Sun et al. [56] studied the effect of grain refinement on tensile properties and deformation twinning behavior of a high-entropy alloy. The results showed that grain refinement

inhibited twinning formation, and the relationship between the critical stress of twinning formation and grain size was given by Equation (4).

$$\sigma_T = m\frac{\gamma}{b_p} + \frac{k_T}{\sqrt{d}} \tag{4}$$

where m is the Taylor factor; γ is the stacking fault energy; b_p is the Burgers vector of a partial dislocation; k_T is the Hall–Petch constant for twinning; and d is the grain size.

For coarse-grained structures, the critical stress of twin formation is small during tensile deformation. For fine-grained structures, the strengthening effect of grain refinement is less than the influence of the critical stress of twin formation caused by grain refinement during tensile deformation. The stress of the fine-grained structure during tensile deformation is less than the critical stress of twin formation, and there will be no deformed twins.

2.3. Deformation Parameters

The deformation parameters, such as temperature, strain, and strain rate, have significant effects on the flow behavior and microstructure of high manganese steel during mechanical processing, and they will further affect their mechanical properties [57,58]. The hot deformation behavior of Fe–25Mn–3Si–3Al TWIP steel was studied, and the constitutive equation related to the Zener–Hollomon parameter (Z) and hot deformation activation energy was established [59]. A strain-dependent constitutive equation for Fe–21Mn–2.5Si–1.5Al steel was put forward, which can accurately estimate the flow stress in the relevant temperature range [60].

Pozdniakov et al. [61] reported that hot deformation could result in a decrease of the grain size. The low stress and ultimate tensile strength decreased with increased deformation temperature, while the plasticity properties of steel were improved, owing to dynamic recrystallisation processes in the austenite phase. Reed et al. [62] found that the change of yield strength with temperature followed an exponential law in stable austenitic steels. The relationship between austenitic strength and temperature may be expressed by Equation (5) when the austenitic strength is determined by the dislocation slip mechanism.

$$\sigma = \sigma_0 exp(-BT) \tag{5}$$

where the parameter B is a function of steel composition, and T is temperature.

It is reported that the grain size increases, and the yield strength and the ultimate tensile strength decrease with an increased rolling temperature [63]. The yield strength of Fe–Mn–C steels decreases faster below room temperature, and it decreases slowly when the deformation temperature is higher than room temperature [19,39]. Kim et al. [9] studied the mechanical properties of Fe–0.4C–(22–26)Mn steel at room temperature and low temperature. The experimental results are shown in Table 3. The research showed that Fe–0.4C–(22–26)Mn steel had a higher yield strength at a low temperature. However, the elongation of Fe–0.4C–(24–26)Mn steel at room temperature was similar to that at a low temperature. Kliber et al. [64] studied TWIP steels with 17 wt.% to 20 wt.% manganese between 900 °C and 1100 °C. The results showed that flow stresses reduced from 300 MPa to 160 MPa with increased temperature.

Table 3. Mechanical properties of Fe–0.4C–(22–26)Mn steel at room temperature and −196 °C (Reprinted with permission from Ref. [9], Copyright 2022 Elsevier).

Temperature (°C)	Steel	Yield Strength (MPa)	Ultimate Tensile Strength (MPa)	Elongation (%)
25	22Mn	334	879	103
	24Mn	314	843	107
	26Mn	322	802	101
−196	22Mn	528	1338	67
	24Mn	574	1288	102
	26Mn	598	1275	110

The mechanical properties of cold-worked high manganese steel can be adjusted by annealing [65–68]. Dislocations and twin grain boundaries can act as nucleation sites for recrystallization during annealing [69,70]. The grain is gradually refined, thus improving the plasticity and toughness of steel with the increase of annealing temperature. Tewary et al. [66] found that recovery occurred in Fe–21Mn–3Si–3Al–0.06C TWIP steels at 600 °C to 800 °C, while recrystallization happened at 900 °C. The ductility of steel was improved, and the tensile strength decreased after annealing at 600 °C. The recrystallization of austenitic high manganese steels containing over 20 wt.% manganese started at about 600 °C [71]. Kim et al. [68] reported that there was more reversed austenite in austenitic stainless steels with increasing the annealing time, which would lead to the decrease of hardness and strength and the increase of elongation. Yuan et al. [72] studied the influence of the annealing temperature on mechanical properties and microstructures of 25Mn–3Cr–3Al–0.3C–0.01N steel. The results showed that annealing temperature had a great influence on the grain size and mechanical properties of steel. The occurrence frequency of the $\sum 3$ grain boundary and deformation twin was closely related to the annealing temperature. The grain size increased from 2.2 μm to 28.7 μm as the annealing temperature increased from 700 °C to 1000 °C. The yield strength and tensile strength decreased by 315 MPa and 290.5 MPa, respectively, and the elongation increased by 21%.

The strain also affects the microstructure evolution of steel. The microstructure changes from a high-density dislocation to a slip band during tensile deformation with the improvement of strain, and deformation twins will be produced. The low-angle grain boundary increases with an increased strain [72]. The recrystallization kinetics are accelerated, and recrystallization grains are refined with the increase of cold-rolling deformation [73]. Tewary et al. [65,66] studied the influence of reduction in cold rolling on the mechanical properties of high manganese steel. The results showed that a larger reduction in cold rolling was beneficial to the hardness, yield strength, and tensile strength of specimens but unfavorable to elongation. It was mainly caused by the crushing and flattening of the austenite phase in the deformation process. The volume fraction of residual austenite decreased with increased deformation [68]. However, Shen et al. [74] reported that the excessive reduction was detrimental to the ductility of steel, and steel products with good yield strength and ductility were obtained by 10% reduction in the cold rolling of Fe–30Mn–3Si–4Al–0.093C steel, with reduction levels of 10% to 70%. Behjati [67] reported that a relatively small reduction of 35% and annealing time of 100 s could provide efficient grain refinement for high manganese austenitic steel and get excellent strength-ductility properties. The yield strength was 890 MPa, the tensile strength was 1340 MPa, and elongation was 41%.

The flow stress of material is sensitive to strain rate. A higher energy will be stored in materials at higher strain rates, which will cause the grain boundary to migrate at a larger speed. It will accelerate the nucleation of dynamic recrystallization grains and increase the frequency of twinning. The grain boundary migration time is prolonged at lower strain rates. It is beneficial to the growth of dynamic recrystallization grains and the nucleation of annealing twins. However, sluggish recrystallization kinetics and annealing twins evolution are observed at intermediate strain rates due to insufficient storage energy and insufficient time for grain boundary migration [75].

Koyama et al. [34] studied the effect of strain rate on the tensile properties of Fe–33Mn–1.1C steel. The research showed that the strength was kept relatively stable, but the elongation increased with the increase of the strain rate when the strain rate was between 10^{-5} s^{-1} and 10^{-2} s^{-1}. Liang et al. [23] studied the static tensile deformation and dynamic tensile deformation behavior of Fe–18Mn–0.6C–1.5Al–0.8Si steel in the strain range of 5.7×10^{-4} s^{-1} to 5.8×10^{-3} s^{-1} and between 55 s^{-1} and 3000 s^{-1} by using a hydraulic tensile testing machine and Hopkinson compression bar tensile testing device, respectively. The results showed that the yield strength of Fe–18Mn–0.6C–1.5A1–0.8Si steel increased significantly from 500 MPa to 727 MPa with an increased strain rate. The maximum flow stress of manganese TWIP steel increased by 50 MPa when the strain rate increased from 5 s^{-1} to 100 s^{-1} [64].

3. Reasons for Deterioration of Low-Temperature Properties

As a material applied in low temperature environments, the high manganese austenitic steel requires not only high strength, but also excellent ductility and toughness to ensure the safety and integrity of materials. The inhibition of brittle fracture at low temperatures is the key factor to improve the low-temperature performance of high manganese steel. The main reasons for the deterioration of low-temperature properties are martensite transformation during low-temperature deformation [10–12], "slipping-off" fracture caused by dislocation accumulation at grain boundaries [13,14], the influence of hydrogen embrittlement [15,16], and the segregation of impurity elements at grain boundaries, etc. [17].

3.1. Martensite Transformation

The low-temperature toughness of high manganese austenitic steel is significantly affected by ε martensite. The interaction between ε martensite, ε martensite and the annealing twin, and grain boundaries often leads to the brittle fracture of high manganese steel at low temperature [10–12]. Figure 6 shows the X-ray diffraction analysis of Fe–17Mn–0.6C steel with 10% strain in the temperature between 173 K and 294 K [10]. It indicated that there was more ε martensite transformation with a decreased temperature.

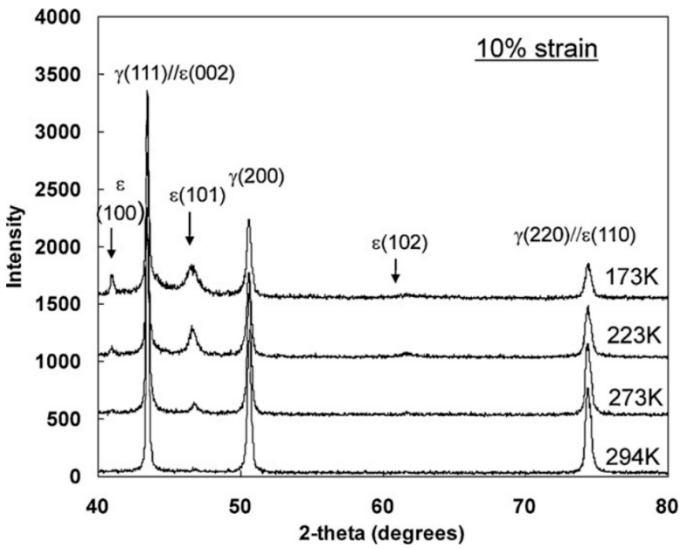

Figure 6. The X-ray diffraction of the Fe–17Mn–0.6C alloy in the temperature range of 173–294 K (Reprinted with permission from Ref. [10], Copyright 2022 Elsevier).

The deformation mechanism of Fe–Mn–C austenitic steel is directly related to temperature and stacking fault energy. Martensite transformation easily occurs when stacking fault energy is low or the plastic deformation enters the high deformation range [76,77]. Alain et al. [77] found that the mechanical martensitic transformation of Fe–22Mn–0.6C steel occurred below 18 $mJ \cdot m^{-2}$. Twinning plays a leading role when the stacking fault

energy is between 12 mJ·m^{-2} and 35 mJ·m^{-2}. Under the ideal state, the stacking fault energy can be calculated according to Equation (6) [12].

$$\gamma_{SFE} = 2\rho\Delta G^{\gamma\to\varepsilon} + 2\sigma_{\text{inter}} \tag{6}$$

where ρ is the molar density along the {111} crystal plane, $\Delta G^{\gamma\to\varepsilon}$ is the molar Gibbs free energy of $\gamma \to \varepsilon$ transformation, and σ_{inter} is the interface energy between the γ and ε phases. The value of σ_{inter} is generally taken between 5 mJ·m^{-2} and 15 mJ·m^{-2} for transition metals [78–80]. The ρ is determined geometrically by introducing the lattice parameter a of the alloy and can be expressed as Equation (7) [77]:

$$\rho = \frac{4}{\sqrt{3}}\frac{1}{a^2 N} \tag{7}$$

where N is Avogadro constant. Olson and Cohen [79,80] added an excess term related to grain size (ΔG_{ex}) into the stacking fault energy, as shown in Equations (8) and (9).

$$\gamma_{SFE} = 2\rho\Delta G^{\gamma\to\varepsilon} + 2\sigma^{\gamma\to\varepsilon} + 2\rho\Delta G_{\text{ex}} \tag{8}$$

$$\Delta G_{ex} = 170.06\exp\left(\frac{-d}{18.55}\right) \tag{9}$$

The above research shows that the decrease of stacking fault energy at lower temperatures can reduce martensite transformation, while grain refinement can effectively compensate the decrease of stacking fault energy caused by a lower temperature and inhibit martensite transformation. The grain refinement increases the strength. However, the plasticity decreases due to the reduction of the work-hardening ability. Takaki et al. [81] studied the tensile properties of an Fe–15Mn alloy with different grain sizes and found that the ε martensite transformation was almost completely inhibited when the grain size decreased below 10 μm. The study of the Fe–17Mn–0.6C alloy showed that the brittle fracture occurred at −150 °C when the grain size was between 10 μm and 37 μm [82]. However, the brittle fracture was restrained when the grain size was refined to 3.5 μm. Tomota et al. [13] found that no ε martensite transformation was found at room temperature when the manganese content increased to 36%, and only 4.2% ε martensite was found at −196 °C when the tensile strain exceeded 60%.

The $\gamma\to\varepsilon$ transformation is also related to the composition of steels. Sato et al. [83] studied the effect of aluminum on the $\gamma\to\varepsilon$ transformation of Fe–(20 and 30)Mn–(0 to 7) Al alloys. The results showed that the $\gamma\to\varepsilon$ transformation temperature decreased when aluminum was added into Fe–20Mn steels. However, the addition of aluminum suppressed the $\gamma\to\varepsilon$ transformation in Fe–30Mn steels. Phase transformations could also be inhibited by adding chromium and nitrogen in Fe–Mn–C steels [84]. There was no α' martensite in the steel with 7.5 wt.% chromium, which resulted in a better ductility [84].

3.2. Slipping-off Fracture

Although high manganese austenitic steel has a complete face-centered cubic structure, the stacking fault will decrease with the decrease of temperature, which will promote the generation of twins and the plane slip of dislocation. During the deformation process, the loose planer dislocations will produce "slipping-off" at the annealed twins boundary or large-angle grain boundary, resulting in brittle fracture [13,14]. Figure 7 shows the slipping-off mechanism of the brittle fracture schematically.

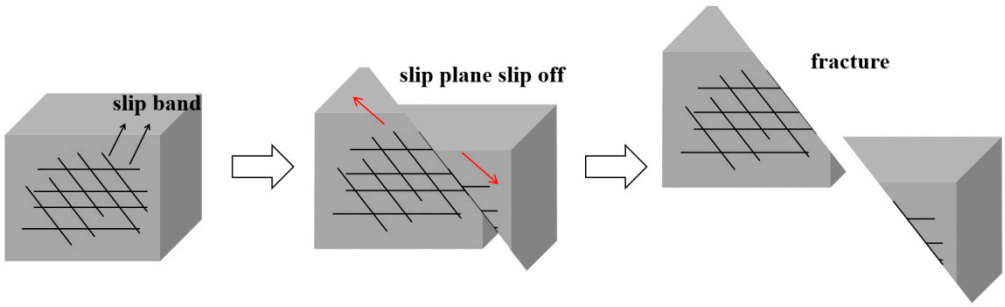

Figure 7. Schematic diagram of the brittle fracture slipping-off mechanism.

The stacking fault energy increases with the decrease of grain size and decreases with the decrease of temperature. Grain refinement can compensate for the influence of decreasing temperature on the reduction of stacking fault energy to a great extent. Metals with a high stacking fault energy are more conducive to the formation of dislocation cells rather than loose planer dislocations in the initial stage of deformation. The dislocation cells formed in the process of deformation will eventually form dislocation cells with a small orientation difference and nanometer level through dynamic refinement, which can prevent the "slipping-off" mechanism that causes brittle fracture.

3.3. Hydrogen Embrittlement

Hydrogen embrittlement caused by the accumulation of a small amount of hydrogen atoms in high-stress areas of materials (such as metal defects) is considered to be a very important factor causing premature fracture. It affects almost all metals and alloys. Bia [15] and Park [16] studied the effect of hydrogen on the tensile process of Fe–31Mn–31Al–3Si and Fe–18Mn–0.6C steels, respectively. It was found that hydrogen charging had little effect on the yield strength of coarse-grained and fine-grained samples, but obviously deteriorated the elongation of coarse-grained samples. Tuluca et al. [85] studied the effect of electrochemical hydrogen charging on the mechanical properties of Fe–33Mn–1.1C austenitic steel with high carbon concentration and a high stacking fault energy. The results showed that the yield strength increased due to the solution hardening of hydrogen. However, the elongation and work-hardening capability decreased. Both intergranular and transgranular fracture, regionally, were detected. The initiation and propagation of hydrogen-assisted crack were the plasticity-dominated mechanisms based on strain localization. The schematic diagram of the hydrogen embrittlement mechanism is shown in Figure 8.

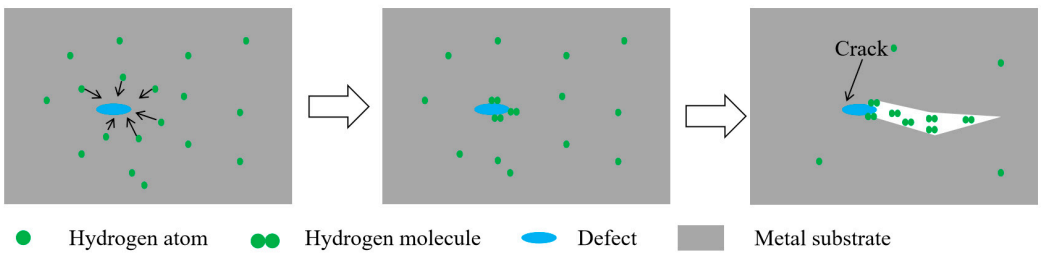

Figure 8. Schematic diagram of hydrogen embrittlement.

Grain refinement could effectively restrain the effect of hydrogen embrittlement. Therefore, the ductile–brittle transition could be suppressed by grain refinement, thus improving the resistance to hydrogen embrittlement [15,16]. Hydrogen embrittlement resistance increases with grain refinement due to the reduced local strain position and crack initiation position, which are hydrogen diffusion channels [86]. Nano-twinned grains in a high carbon manganese steel can decrease the hydrogen diffusivity through the bulk

material, reduce dislocations glide during plastic deformation, and increase the resistance to hydrogen embrittlement [87].

The composition of high manganese steel has a certain influence on its hydrogen embrittlement sensitivity. The hydrogen embrittlement sensitivity increases with increased diffusible hydrogen content [11]. The solubility of hydrogen increases with increased aluminum in steels [88,89]. Therefore, the hydrogen uptake can be inhibited by adding aluminum in high manganese steel, which is associated with the prevention of hydrogen diffusion. Moreover, it can reduce the embrittlement sensitivity to diffusible hydrogen content [11,90]. Similarly, adding copper in steels could increase the stacking fault energy and inhibit the hydrogen embrittlement sensitivity [91]. However, the effect of aluminum on the hydrogen embrittlement of steels could be inhibited by phosphorus in steels, while the existence of phosphorus in steels without aluminum does not aggravate the hydrogen embrittlement sensitivity of steel [91]. Koyama et al. [92] reported that hydrogen embrittlement was suppressed by the addition of manganese in steels, owing to the decrease the formation trend to twin and martensite. Lee et al. [93] studied the effect of silicon on hydrogen embrittlement of Fe–18Mn–0.6C–xSi TWIP steels. The results showed that the addition of silicon would lead to the formation of ε martensite and is conducive to the occurrence of brittle fracture.

3.4. Segregation of Impurity Element at Grain Boundaries

Alloys and impurity elements can segregate on the surface and grain boundary of metals [94]. The change of local chemical composition at the grain boundary affects the critical stress of twins generation, thus affecting its work-hardening behavior. García-Mazarío et al. [95] characterized the grain boundary microchemical of martensitic steel by Auger electron spectroscopy and found out that step-cooling promoted chromium, molybdenum, and phosphorus segregation to grain boundaries, which would increase the sensitivity of the embrittlement of materials. Helium segregation at grain boundaries was found in irradiated materials. The fracture criteria of material depended upon the time scale of crack growth, the density, and the size of helium segregation [96]. Xue et al. [97] found nonequilibrium segregation of manganese at the grain boundaries in high manganese austenitic Fe–Mn alloys. The segregation increased with increasing manganese content. The ductile-to-brittle transition temperature and intergranular fracture increased with increased manganese content, solid–solution treatment temperature, and cooling rate, which indicated that the intergranular fracture and embrittlement were caused by manganese segregation. Herbig et al. [17] used 3D atom probe tomography technology to study the grain boundary segregation characteristics of Fe–28Mn–0.3C steel containing a 50% general grain boundary and 35% $\sum 3$ annealed twins grain boundary, as shown in Figure 9. The segregation of boron, carbon, phosphorus, and traces of silicon and copper were found on the general grain boundary. The segregation of boron and phosphorus also existed on the grain boundary of $\sum 3$ annealed twins. Although the crystallography of annealed twins was consistent with that of deformed twins, no segregation of elements was found on the deformed twins. Manganese was neither enriched nor depleted on the general grain boundary. The enrichment of the carbon element on the general grain boundary led to the increase of the local stacking fault energy, which increased the forming stress of twins. The depletion of the carbon element on the annealed twins grain boundaries was beneficial to the twins nucleus.

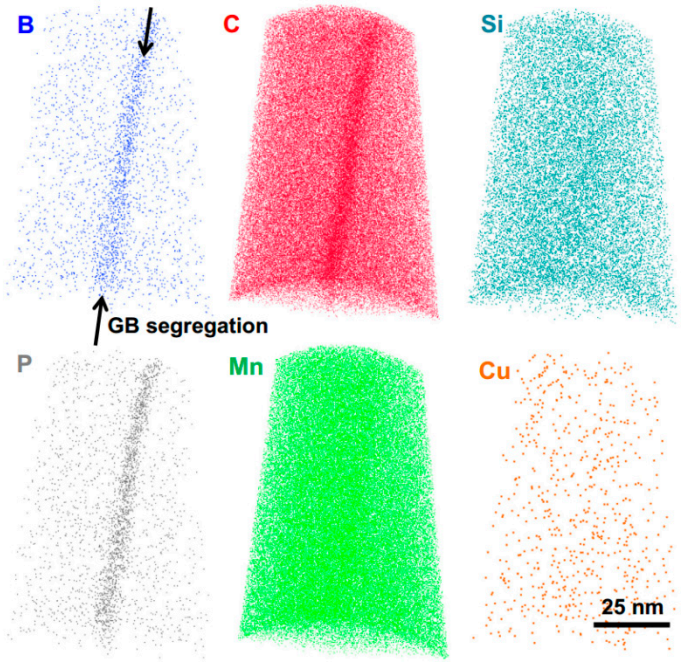

Figure 9. Element segregation on grain boundaries in 3D elemental atom maps (Reprinted with permission from Ref. [17], Copyright 2022 Elsevier).

4. Deformation Mechanisms

Good strength and plasticity is the basis of the high manganese steel application. However, it is difficult to get the strength–plasticity combination of materials. It is always a difficult problem in industry and experimental research to prepare metal materials with high strength and excellent plasticity. In recent years, a breakthrough for keeping high strength and good plasticity has been achieved through different deformation mechanisms, including the TRIP effect, TWIP effect, SIP effect, and MBIP effect, etc.

4.1. TRIP Effect

TRIP is an important deformation strengthening mechanism in high manganese steels to obtain excellent properties combining high strength and good ductility. Metastable austenite is transformed into ε martensite or induced α' martensite when the strain exceeds a certain level in tensile deformation. Martensite transformation can lead to a decrease in the grain size and fine-grain strengthening [98]. In addition, martensite, as the second phase, strengthens the original austenitic material, which shows an increase in strength. The appearance of martensite during stretching increases the work hardening rate, delays the occurrence of necking, and improves the uniform elongation of material. Therefore, the TRIP effect of strain-induced martensite simultaneously improves the strength and plasticity of material [24]. The transformation from residual austenite to martensite belongs to non-diffusion transformation. The martensite produced by the residual austenite transformation can produce the TRIP effect, while that obtained by deformation and quenching has no transformation toughness. El-Sherbiny et al. [99] found the content of residual austenite increased with the increase of manganese. Manganese content has an important influence on the phase transformation of high manganese steel. Li et al. [100] reported that $\gamma \rightarrow \varepsilon$, $\varepsilon \rightarrow \alpha'$ and $\gamma \rightarrow \alpha'$ could occur in steel with 15 wt.% manganese. However, there was a larger amount of ε martensite in steel when the content of manganese increased to 19 wt.%. Manganese in steels could stabilize austenite and ε martensite, and the grain refinement of the TRIP effect mainly resulted from the $\gamma \rightarrow \varepsilon$, rather than the $\gamma \rightarrow \alpha'$, transformation [101].

4.2. TWIP Effect

In addition to the TRIP effect, the TWIP effect is another deformation mechanism to obtain an excellent strength–ductility balance material. The stress increases continuously, and some oriented grains produce deformation twins with the increase of strain during tensile deformation. Deformation twinning and twin intersection will appear in more grains when the stress exceeds the critical stress of twinning. Deformation twins and twin intersection divide the original austenite grains and refine them. The strength of material is improved by dynamic fine grain strengthening. The average free path of the dislocation slip is reduced, the work hardening rate is increased, the occurrence of necking is delayed, and the plasticity of material is improved by dividing the original austenite grain. Therefore, the strength and plasticity of material is increased by the TWIP effect [20]. Grässel et al. [39] found that Fe–25Mn–3Si–3Al TWIP steel had a moderate tensile strength of about 650 MPa and high uniform elongation of about 80% at room temperature due to the formation of massive twinning during deformation.

The TRIP effect is more beneficial to increase the strength of material, and the TWIP effect is more conducive to improving the ductility of material [40,45]. The deformation mechanism of steels can change between the TRIP effect and TWIP effect under different conditions. Eskandari et al. [101] studied the mechanical behavior of austenitic steel with 21 wt.% manganese at 25 °C to 1000 °C. The results showed both deformation-induced martensite and mechanical twinning were observed in the steel at 25 °C to 100 °C. However, there was little mechanical twinning when the temperature rose above 200 °C, indicating that the deformation mechanism changed to TWIP [101].

4.3. SIP Effect

Frommeyer et al. [25] studied the plastic deformation behavior of Fe–28Mn–10Al–1.2C steel, and the SIP effect was introduced to explain the results. They found that the nano-scale κ carbide with austenite could undergo shear deformation during the deformation process, thus hindering the dislocation movement and increasing the deformation resistance, which made the experimental steel show a good uniform deformation ability and high tensile strength during the tensile deformation. Moreover, an obvious plane slip shear band was observed in the microstructure after deformation. Choi et al. [102] obtained κ carbides with different sizes and volume fractions through different aging treatments and analyzed their effects on the deformation behavior and mechanical properties of Fe–Mn–Al austenitic steel. It was found that austenite with a high stacking fault energy showed plane slip characteristics owing to the existence of ordered κ carbide. Dislocation passed through κ carbide in the movement process, forming a large number of slip bands. It showed plane slip characteristics instead of a dislocation cellular structure.

4.4. MBIP Effect

Yoo et al. [26] studied the microstructure evolution of Fe–28Mn–10Al–1.0C austenite steel during tensile deformation at room temperature, and they put forward the MBIP theory to explain the combination of high strength and toughness of the steel. The research object was a single-phase austenite structure after plastic deformation and solution treatment. The alloy elements were completely dissolved in the austenite matrix, the stacking fault energy of austenite was 85 $mJ \cdot m^{-2}$ at room temperature, and the free energy difference between austenite and martensite was about 1130 $J \cdot mol^{-1}$. Neither the TRIP effect nor TWIP effect occurred with the increase of strain. However, a large number of micro-band structures were formed. They crossed each other, showing obvious plane slip characteristics. The continuous strain hardening of austenite resulted in a good match between strength and plasticity. The tensile strength of the steel was 843 MPa, and the elongation after fracture was 100%.

In the tensile deformation process of metals with a low stacking fault energy, the total dislocations are easily decomposed into partial dislocations, which are wide in width and small in lattice distortion, and it is difficult to cross-slip. Therefore, the dislocation

movement is confined to a single slip surface. The dislocation density increases with the increase of strain, and a large number of dislocations pile up to gradually form dislocation clusters, a Taylor lattice, high-density dislocation walls, domain boundaries, and other structures, resulting in MBIP deformation [103]. The deformation mechanisms of both MBIP and SIP belong to the plane slip.

Gutierrez et al. [104] thought that the formation of a micro-band was due to the strong plastic deformation confined to the single or coplanar slip system, while the dislocation motion in the second non-coplanar slip system was limited. Therefore, this highly localized microstructure was considered to be a softening mechanism instead of a strengthening mechanism. The micro-band was a narrow shear zone within the grain surrounded by a certain geometric structure. Different dislocation substructures, such as a high-density dislocation wall and Taylor lattice, could also be observed. However, the effect of these different dislocation structures on the strain strengthening ability of Fe–Mn–Al steel was not clear.

The deformation mechanism of austenite mainly depends on the stacking fault energy [105,106]. The deformation mechanism is mainly TRIP when the Gibbs free energy difference between austenite and martensite is less than -220 J·mol^{-1} and when the stacking fault energy is less than 25 mJ·m^{-2}. The dominant deformation mechanism of austenite is TWIP when the stacking fault energy is 25–55 mJ·m^{-2}. When the stacking fault energy is greater than 55 mJ·m^{-2}, the deformation mechanism is mainly SIP or MBIP [105]. The stacking fault energy of steels is related to the composition and deformation temperature. Therefore, the deformation mechanism of high manganese austenitic steel can be controlled through reasonable composition control and optimization of the deformation temperature.

5. Conclusions

This review covers the research progress of high manganese austenitic steel, including factors affecting the mechanical performance, the deterioration at low temperatures, and deformation mechanisms.

The mechanical properties of steels are related to the chemical composition; grain size; and deformation parameters, such as temperature, strain, and strain rate. The strength of high manganese austenitic steel increases with increased carbon, aluminum, and nitrogen elements in steel. Niobium alloying is harmful to the cryogenic impact on toughness and tensile toughness of steel, while the addition of aluminum is beneficial to toughness. Silicon will promote martensite transformation during deformation. Grain refinement can improve the strength of high manganese austenitic steel without affecting its low temperature plasticity and toughness. The effect of grain refinement on the yield strength at -196 °C is stronger than that at 25 °C. The grain can be changed by controlling deformation parameters. It is refined with the increase of deformation, while the grain size increases with an increased rolling and annealing temperature. The yield strength of high manganese steel decreases, and the plasticity gradually increases with increased deformation temperature. The elongation of steel increases with the increase of strain rate, while there is little effect on the strength.

The brittle fracture at a low temperature is an important reason for the failure of high manganese austenitic steel. It can be caused by martensite transformation of high manganese austenitic steel and segregation of the impurity element at grain boundaries. The martensite transformation can be suppressed by adding aluminum, chromium, and nitrogen in steels. Moreover, the loose planer dislocations produced in the deformation process will result in "slipping-off" at the annealed twins boundary or large-angle grain boundary, which promotes the brittle fracture. "Slipping-off" can be prevented by increasing the stacking fault energy of steel. Hydrogen embrittlement is harmful to the ductility of steel, and it can also cause a fracture of steel. Hydrogen embrittlement sensitivity is related to the grain size and the composition of steels. It can be effectively restrained by grain refinement; increasing the content of aluminum, copper, and manganese in steel; and decreasing the phosphorus and silicon.

The excellent strength–ductility combination of high manganese austenitic steel is beneficial to the application in liquefied natural gas storage tanks. The strength and ductility of materials can be optimized by the TRIP effect, TWIP effect, SIP effect, and MBIP effect. The deformation mechanism of high manganese austenitic steel depends on the stacking fault energy, which is related to the composition and deformation temperature. The TRIP effect plays a major role when the stacking fault energy is less than 25 $mJ \cdot m^{-2}$. The deformation mechanism is TWIP when the stacking fault energy is between 25 $mJ \cdot m^{-2}$ and 55 $mJ \cdot m^{-2}$, and it changes to the SIP effect and MBIP effect with the stacking fault energy increases to larger than 55 $mJ \cdot m^{-2}$.

Author Contributions: Conceptualization, Z.J. and L.Y.; methodology, L.X. and H.Z.; validation, Y.L. and Z.J.; writing—original draft preparation, L.X.; writing—review and editing, Y.L. and G.L.; visualization, L.X. and H.Z.; supervision, Y.L.; project administration, L.X. and L.Y.; funding acquisition, L.X. and L.Y. All authors have read and agreed to the published version of the manuscript.

Funding: This research was funded by the University of Science and Technology Liaoning Talent Project Grants (No. 601010314), the Liaoning Province Doctoral Research Start-up Fund Plan Project (No. 2021-BS-243), and the State Key Laboratory of Metal Material for Marine Equipment and Application, University of Science and Technology Liaoning Co., project (No. HGSKL-USTLN(2021)08).

Data Availability Statement: Not applicable.

Conflicts of Interest: The authors declare no conflict of interest.

References

1. Liu, D.F.; Yang, X.L.; Hou, L.F.; Cui, T.X.; Wei, Y.H. Research and application of ultralow temperature 9Ni steel for LNG storage tank. *J. Iron Steel Res.* **2009**, *21*, 1–5.
2. Shinji, Y.; Carlo, A.; Yukio, M. Impact tensile properties of nine per cent nickel steel. *J. Soc. Mater. Sci. Jpn.* **1997**, *46*, 1286–1292.
3. Kinney, C.C.; Pytlewski, K.R.; Khachaturyan, A.G.; Morris, J.W. The microstructure of lath martensite in quenched 9Ni steel. *Acta Mater.* **2014**, *69*, 372–385. [CrossRef]
4. Hichem, M.; Ali, H.; Khadîdja, B. Effects of niobium and molybdenum on microstructures after hardening and wear resistance of austenitic manganese steel. *Chem. Mater. Res.* **2013**, *5*, 1–5.
5. Koyama, M.; Akiyama, E.; Lee, Y.K.; Raabe, D.; Tsuzaki, K. Overview of hydrogen embrittlement in high-Mn steels. *Int. J. Hydrog. Energ.* **2017**, *42*, 12706–12723. [CrossRef]
6. Wang, X.J.; Sun, X.J.; Song, C.; Chen, H.; Han, W.; Pan, F. Enhancement of yield strength by chromium/nitrogen alloying in high-manganese cryogenic steel. *Mater. Sci. Eng. A* **2017**, *698*, 110–116. [CrossRef]
7. Sohn, S.S.; Hong, S.; Lee, J.; Suh, B.C.; Kim, S.K.; Lee, B.J.; Kim, N.J.; Lee, S. Effects of Mn and Al contents on cryogenic-temperature tensile and Charpy impact properties in four austenitic high-Mn steels. *Acta Mater.* **2015**, *100*, 39–52. [CrossRef]
8. Lee, J.; Sohn, S.S.; Hong, S.; Suh, B.C.; Kim, S.K.; Lee, B.J.; Kim, N.J.; Lee, S. Effects of Mn addition on tensile and Charpy impact properties in austenitic Fe-Mn-C-Al-based steels for cryogenic applications. *Metall. Mater. Trans. A* **2014**, *45*, 5419–5430. [CrossRef]
9. Kim, H.; Ha, Y.; Kwon, K.H.; Kang, M.; Kim, N.J.; Lee, S. Interpretation of cryogenic-temperature Charpy impact toughness by microstructural evolution of dynamically compressed specimens in austenitic 0.4C-(22-26)Mn steels. *Acta Mater.* **2015**, *87*, 332–343. [CrossRef]
10. Koyama, M.; Sawaguchi, T.; Lee, T.; Lee, C.S.; Tsuzakiet, K. Work hardening associated with ε-martensitic transformation, deformation twinning and dynamic strain aging in Fe-17Mn-0.6C and Fe-17Mn-0.8C TWIP steels. *Mater. Sci. Eng. A* **2011**, *528*, 7310–7316. [CrossRef]
11. Chun, Y.S.; Park, K.T.; Chong, S.L. Delayed static failure of twinning-induced plasticity steels. *Scr. Mater.* **2012**, *66*, 960–965. [CrossRef]
12. Curtze, S.; Kuokkala, V.T. Dependence of tensile deformation behavior of TWIP steels on stacking fault energy, temperature and strain rate. *Acta Mater.* **2010**, *58*, 5129–5141. [CrossRef]
13. Tomota, Y.; Xia, Y.; Inoue, K. Mechanism of low temperature brittle fracture in high nitrogen bearing austenitic steels. *Acta Mater.* **1998**, *46*, 1577–1587. [CrossRef]
14. Wang, W.; Wang, S.; Yang, K.; Shan, Y. Temperature dependence of tensile behavior of a high nitrogen Fe-Cr-Mn-Mo stainless steel. *Mater. Des.* **2009**, *30*, 1822–1824. [CrossRef]
15. Bai, Y.; Momotani, Y.; Chen, M.C.; Shibata, A.; Tsuji, N. Effect of grain refinement on hydrogen embrittlement behaviors of high-Mn TWIP steel. *Mater. Sci. Eng. A* **2016**, *651*, 935–944. [CrossRef]
16. Park, I.J.; Lee, S.M.; Jeon, H.H.; Lee, Y.K. The advantage of grain refinement in the hydrogen embrittlement of Fe-18Mn-0.6C twinning-induced plasticity steel. *Corros. Sci.* **2015**, *93*, 63–69. [CrossRef]

17. Herbig, M.; Kuzmina, M.; Haase, C.; Marceau, R.K.W.; Gutierrez-Urrutia, I.; Haley, D.; Molodov, D.A.; Choi, P.; Raabe, D. Grain boundary segregation in Fe-Mn-C twinning-induced plasticity steels studied by correlative electron backscatter diffraction and atom probe tomography. *Acta Mater.* **2015**, *83*, 37–47. [CrossRef]
18. Wang, H.H.; Luo, Q.; Wan, X.L.; Li, L.; Misra, R.D.K. Design of novel Fe-Mn-Ni cryogenic steel: Microstructure-property relationship during simulated welding. *Sci. Technol. Weld. Join.* **2018**, *23*, 125–133. [CrossRef]
19. Bouaziz, O.; Allain, S.; Scott, C.P.; Cugy, P.; Barbier, D. High manganese austenitic twinning induced plasticity steels: A review of the microstructure properties relationships. *Curr. Opin. Solid State Mater. Sci.* **2011**, *15*, 141–168. [CrossRef]
20. De Cooman, B.C.; Estrin, Y.; Kim, S.K. Twinning-induced plasticity (TWIP) steels. *Acta Mater.* **2018**, *142*, 283–362. [CrossRef]
21. Dini, G.; Najafizadeh, A.; Ueji, R.; Monir-Vaghefi, S.M. Tensile deformation behavior of high manganese austenitic steel: The role of grain size. *Mater. Des.* **2010**, *31*, 3395–3402. [CrossRef]
22. Ueji, R.; Tsuchida, N.; Terada, D.; Tsuji, N.; Tanaka, Y.; Takemura, A.; Kunishige, K. Tensile properties and twinning behavior of high manganese austenitic steel with fine-grained structure. *Scr. Mater.* **2008**, *59*, 963–966. [CrossRef]
23. Liang, Z.Y.; Wang, X.; Huang, W.; Huang, M.X. Strain rate sensitivity and evolution of dislocations and twins in a twinning-induced plasticity steel. *Acta Mater.* **2015**, *88*, 170–179. [CrossRef]
24. Azrin, M.; Olson, G.B.; Gagne, R.A. Inhomogenous deformation and strain-rate effects in high-strength TRIP steels. *Mat. Sci. Eng.* **1976**, *23*, 33–41. [CrossRef]
25. Frommeyer, G.; Brüx, U. Microstructures and mechanical properties of high-strength Fe-Mn-Al-C light-weight TRIPLEX steels. *Steel Res. Int.* **2006**, *77*, 627–633. [CrossRef]
26. Yoo, J.D.; Hwang, S.W.; Park, K.T. Origin of extended tensile ductility of a Fe-28Mn-10AI-1C steel. *Metall. Mater. Trans. A* **2009**, *40*, 1520–1523. [CrossRef]
27. Tofaute, W.; Linden, K. Transformations in solid state of manganese steels containing to 1.2% C and 17% Mn. *Arch. Eisenhuttenwes* **1936**, *10*, 515.
28. Saeed-Akbari, A.; Imlau, J.; Prahl, U.; Bleck, W. Derivation and variation in composition-dependent stacking fault energy maps based on subregular solution model in high-manganese steels. *Metall. Mater. Trans. A* **2009**, *40*, 3076–3090. [CrossRef]
29. Wietbrock, B.; Xiong, W.; Bambach, M.; Hirt, G. Effect of temperature, strain rate, manganese and carbon content on flow behavior of three ternary Fe-Mn-C (Fe-Mn23-C0.3, Fe-Mn23-C0.6, Fe-Mn28-C0.3) high-manganese steels. *Steel Res. Int.* **2011**, *82*, 63–69. [CrossRef]
30. Chen, L.; Yang, Z.; Qin, X. Some aspects of high manganese twinning-induced plasticity (TWIP) steel, a review. *Acta Metall. Sin. (Engl. Lett.)* **2013**, *26*, 1–15. [CrossRef]
31. Bouaziz, O. Strain-hardening of twinning-induced plasticity steels. *Scr. Mater.* **2012**, *66*, 982–985. [CrossRef]
32. Lee, S.J.; Han, J.; Lee, S.; Kang, S.H.; Lee, S.M.; Lee, Y.K. Design for Fe-high Mn alloy with an improved combination of strength and ductility. *Sci. Rep.* **2017**, *7*, 3573. [CrossRef] [PubMed]
33. Ghasri-Khouzani, M.; Mcdermid, J.R. Effect of carbon content on the mechanical properties and microstructural evolution of Fe-22Mn-C steels. *Mater. Sci. Eng. A* **2015**, *621*, 118–127. [CrossRef]
34. Koyama, M.; Shimomura, Y.; Chiba, A.; Akiyama, E.; Tsuzaki, K. Room-temperature blue brittleness of Fe-Mn-C austenitic steels. *Scr. Mater.* **2017**, *141*, 20–23. [CrossRef]
35. Wang, X.; Zurob, H.S.; Embury, J.D.; Ren, X.; Yakubtsov, I. Microstructural features controlling the deformation and recrystallization behaviour Fe-30%Mn and Fe-30%Mn-0.5%C. *Mater. Sci. Eng. A* **2010**, *527*, 3785–3791. [CrossRef]
36. Ghasrikhouzani, M.; Mcdermid, J.R. Microstructural evolution and mechanical behaviour of Fe-30Mn-C steels with various carbon contents. *Mater. Sci. Eng.* **2017**, *33*, 1159–1170.
37. Bouaziz, O.; Zurob, H.; Chehab, B.; Embury, J.D.; Allain, S.; Huang, M. Effect of chemical composition on work hardening of Fe-Mn-C TWIP steels. *Mater. Sci. Eng.* **2011**, *27*, 707–709. [CrossRef]
38. Saeed-Akbari, A.; Schwedt, A.; Bleck, W. Characterization and prediction of flow behavior in high-manganese twinning induced plasticity steels, Part I. Mechanism maps and work-hardening behavior. *Metall. Mater. Trans. A* **2012**, *43*, 1688–1704. [CrossRef]
39. Grässel, O.; Krüger, L.; Frommeyer, G.; Meyer, L.W. High strength Fe-Mn-(Al, Si) TRIP/TWIP steels development-properties-application. *Int. J. Plast.* **2000**, *16*, 1391–1409. [CrossRef]
40. Torabinejad, V.; Zareihanzaki, A.; Sabet, M.; Abedi, H.R. The effect of low temperature annealing on the mechanical behavior of cold rolled dual-phase twinning-induced plasticity steel. *Mater. Des.* **2011**, *32*, 2345–2349. [CrossRef]
41. Charles, J.; Berghézan, A.; Lutts, A. Structural and mechanical properties of high-alloy manganese-aluminum steels. *Le J. Phys. Colloq.* **1982**, *43*, C4-435.
42. Chen, F.C.; Chou, C.P.; Li, P.; Chu, S.L. Effect of aluminium on TRIP Fe-Mn-Al alloy steels at room temperature. *Mater. Sci. Eng. A* **1993**, *160*, 261–270. [CrossRef]
43. Han, Y.S.; Hong, S.H. The effect of Al on mechanical properties of Fe-32Mn-12Cr-xAl-0.4C cryogenic alloys. *Mater. Sci. Eng. A* **1997**, *222*, 76–83. [CrossRef]
44. Takaki, S.; Furuya, T.; Tokunaga, Y. Effect of Si and Al additions on the low temperature toughness and fracture mode of Fe-27Mn alloys. *ISIJ Int.* **1990**, *30*, 632–638. [CrossRef]
45. Hamada, A.S.; Karjalainen, L.P.; Somani, M.C. The influence of aluminum on hot deformation behavior and tensile properties of high-Mn TWIP steels. *Mater. Sci. Eng. A* **2007**, *467*, 114–124. [CrossRef]
46. Wang, C.J.; Chang, Y.C. NaCl-induced hot corrosion of Fe-Mn-Al-C alloys. *Mater. Chem. Phys.* **2002**, *76*, 151–161. [CrossRef]

47. Eberle, K.; Cantinieaux, P.; Harlet, P. New thermomechanical strategies for the production of high strength low alloyed multiphase steel showing a transformation induced plasticity (TRIP) effect. *Steel Res. Int.* **1999**, *70*, 176–181. [CrossRef]
48. Kwon, Y.J.; Lee, T.; Lee, J.; Chun, Y.S.; Lee, C.S. Role of Cu on hydrogen embrittlement behavior in Fe-Mn-C-Cu TWIP steel. *Int. J. Hydrog. Energy* **2015**, *40*, 7409–7419. [CrossRef]
49. Chen, J.; Ren, J.K.; Liu, Z.Y.; Wang, G.D. The essential role of niobium in high manganese austenitic steel for application in liquefied natural gas tanks. *Mater. Sci. Eng. A* **2020**, *772*, 138733. [CrossRef]
50. Wang, X.J.; Sun, X.J.; Song, C.; Chen, H.; Tong, S.; Han, W.; Pan, F. Evolution of microstructures and mechanical properties during solution treatment of a Ti–V–Mo-containing highmanganese cryogenic steel. *Mater. Charact.* **2018**, *135*, 287–294. [CrossRef]
51. Wang, X.J.; Sun, X.J.; Song, C.; Chen, H.; Tong, S.; Han, W.; Pan, F. Grain size-dependent mechanical properties of a high-manganese austenitic steel. *Acta Metall. Sin. (Engl. Lett.)* **2019**, *32*, 746–754. [CrossRef]
52. Wu, D.; Zhang, J.; Huang, J.C.; Bei, H.; Nieh, G.T. Grain-boundary strengthening in nanocrystalline chromium and the Hall-Petch coefficient of body-centered cubic metals. *Scr. Mater.* **2013**, *68*, 118–121. [CrossRef]
53. Jang, D.; Greer, J.R. Size-induced weakening and grain boundary-assisted deformation in 60 nm grained Ni nanopillars. *Scr. Master.* **2011**, *64*, 77–80. [CrossRef]
54. Lu, J.; Jin, L.; Dong, J.; Zeng, X.Q.; Yao, Z.Y. Deformation behaviors of AZ31 magnesium alloy by equal channel angular extrusion. *Chin. J. Nonferr. Met.* **2009**, *19*, 424–432.
55. Dong, H. *Advanced Steel Material*; Science Press: Beijing, China, 2008.
56. Sun, S.J.; Tian, Y.Z.; Lin, H.R.; Yang, H.J.; Dong, X.G.; Wang, Y.H.; Zhang, Z.F. Transition of twinning behavior in Co Cr Fe Mn Ni high entropy alloy with grain refinement. *Mater. Sci. Eng. A* **2018**, *712*, 603–607. [CrossRef]
57. Li, C.; Ma, B.; Song, Y.; Li, K.; Dong, J. The annealing twins of Fe-20Mn-4Al-0.3C austenitic steels during symmetric and asymmetric hot rolling. *Metals* **2018**, *8*, 882. [CrossRef]
58. Haase, C.; Barrales-Mora, L.A.; Roters, F.; Molodov, D.A.; Gottstein, G. Applying the texture analysis for optimizing thermomechanical treatment of high manganese twinning-induced plasticity steel. *Acta Mater.* **2014**, *80*, 327–340. [CrossRef]
59. Li, D.J.; Feng, Y.R.; Yin, Z.F.; Shangguan, F.S.; Wang, K.; Liu, Q.; Hu, F. Prediction of hot deformation behaviour of Fe-25Mn-3Si-3Al TWIP steel. *Mater. Sci. Eng. A* **2011**, *528*, 8084–8089. [CrossRef]
60. Marandi, A.; Zarei-Hanzaki, A.; Haghdadi, N.; Eskandari, M. The prediction of hot deformation behavior in Fe-21Mn-25.Si-1.5Al transformation-twinning induced plasticity steel. *Mater. Sci. Eng. A* **2012**, *554*, 72–78. [CrossRef]
61. Prosviryakov, A.; Mondoloni, B.; Churyumov, A.; Pozdniakov, A. Microstructure and hot deformation behaviour of a novel Zr-alloyed high-boron steel. *Metals* **2019**, *9*, 218. [CrossRef]
62. Reed, R.P.; Horiuchi, T. Austenitic Steels at Low Temperatures. In Proceedings of the International Cryogenic Engineering Conference, Kobe, Japan, 10 May 1982.
63. Chen, Y.; Zhang, X.; Cai, Z.; Ding, H.; Pan, M.; Wei, W.; Liu, Y. Effects of rolling temperature on the microstructure and mechanical properties of a high-Mn austenitic steel for cryogenic applications. *Steel Res. Int.* **2020**, *91*, 1900660. [CrossRef]
64. Kliber, J.; Drozd, K. Stress-strain behaviour and softening in manganese TWIP steel tested in Thermalmechanical simulator. *Metal* **2009**, *19–21*, 5.
65. Tewary, N.; Ghosh, S.; Bera, S.; Chakrabarti, D.; Chatterjee, S. Influence of cold rolling on microstructure, texture and mechanical properties of low carbon high Mn TWIP steel. *Mater. Sci. Eng. A* **2014**, *615*, 405–415. [CrossRef]
66. Tewary, N.; Ghosh, S.; Chatterjee, S. Effect of annealing on microstructure and mechanical behaviour of cold rolled low C, high Mn TWIP steel. *Int. J. Metall. Eng.* **2015**, *4*, 12–23.
67. Behjati, P.; Kermanpur, A.; Karjalainen, L.; Järvenpää, A.; Jaskari, M.; Baghbadorani, H.S.; Najafifizadeh, A.; Hamada, A. Influence of prior cold rolling reduction on microstructure and mechanical properties of a reversion annealed high-Mn austenitic steel. *Mater. Sci. Eng. A* **2016**, *650*, 119–128. [CrossRef]
68. Kim, Y.; Kim, J.; Hwang, T.; Lee, J.; Kang, C. Effect of austenite on mechanical properties in high manganese austenitic stainless steel with two phase of martensite and austenite. *Met. Mater. Int.* **2015**, *21*, 485–489. [CrossRef]
69. Bracke, L.; Verbeken, K.; Kestens, L.; Penning, J. Microstructure and texture evolution during cold rolling and annealing of a high Mn TWIP steel. *Acta Mater.* **2009**, *57*, 1512–1524. [CrossRef]
70. Haase, C.; Kühbach, M.; Barrales-Mora, L.A.; Wong, S.L.; Roters, F.; Molodov, D.A.; Gottstein, G. Recrystallization behavior of a high-manganese steel: Experiments and simulations. *Acta Mater.* **2015**, *100*, 155–168. [CrossRef]
71. Santos, D.B.; Saleh, A.A.; Gazder, A.A.; Carman, A.; Duarte, D.M.; Ribeiro, É.A.; Gonzalez, B.M.; Pereloma, E.V. Effect of annealing on the microstructure and mechanical properties of cold rolled Fe-24Mn-3Al-2Si-1Ni-0.06C TWIP steel. *Mater. Sci. Eng. A* **2011**, *528*, 3545–3555. [CrossRef]
72. Yuan, X.; Chen, L.; Zhao, Y.; Di, H.; Zhu, F. Influence of annealing temperature on mechanical properties and microstructures of a high manganese austenitic steel. *J. Mater. Process. Technol.* **2015**, *217*, 278–285. [CrossRef]
73. Park, M.; Kang, M.S.; Park, G.W.; Choi, E.Y.; Kim, B.J. The effects of recrystallization on strength and impact toughness of cold-worked high-Mn austenitic steels. *Metals* **2019**, *9*, 948. [CrossRef]
74. Shen, Y.; Qiu, C.; Wang, L.; Sun, X.; Zhao, X.; Zuo, L. Effects of cold rolling on microstructure and mechanical properties of Fe-30Mn-3Si-4Al-0.093 C TWIP steel. *Mater. Sci. Eng. A* **2013**, *561*, 329–337. [CrossRef]
75. Chen, Y.; Zhang, X.M.; Cai, Z.H.; Ding, H.; Li, H.S. Hot deformation behavior of a high-Mn austenitic steel for cryogenic liquified natural gas applications. *J. Mater. Eng. Perform.* **2020**, *29*, 5503–5514. [CrossRef]

76. Kowalska, J.; Kowalski, M. Development of microstructure and texture after cold-rolling Fe-24Mn-3Al-3Si high-manganese steel. *J. Mater. Eng. Perform.* **2020**, *29*, 1495–1501. [CrossRef]
77. Alain, S.; Chateau, J.P.; Bouaziz, O.; Migot, S.; Guelton, N. Correlations between the calculated stacking fault energy and the plasticity mechanisms in Fe-Mn-C alloys. *Mater. Sci. Eng. A* **2004**, *387–389*, 158–162. [CrossRef]
78. Olson, G.B.; Cohen, M. A general mechanism of martensitic nucleation: Part I. General concepts and the FCC → HCP transformation. *Metall. Trans. A* **1976**, *7*, 1897–1904.
79. Lee, Y.K.; Choi, C. Driving force for $\gamma \rightarrow \varepsilon$, martensitic transformation and stacking fault energy of γ, in Fe-Mn binary system. *Metall. Mater. Trans. A* **2000**, *31*, 355–360. [CrossRef]
80. Ferreira, P.J.; Müllner, P. A thermodynamic model for the stacking-fault energy. *Acta Mater.* **1998**, *46*, 4479–4484. [CrossRef]
81. Takaki, S.; Nakatsu, H.; Tokunaga, Y. Effects of austenite grain size on ε martensitic transformation in Fe-15mass%Mn alloy. *Mater. Trans.* **1993**, *34*, 489–495. [CrossRef]
82. Koyama, M.; Lee, T.; Chong, S.L.; Tsuzaki, K. Grain refinement effect on cryogenic tensile ductility in a Fe-Mn-C twinning-induced plasticity steel. *Mater. Des.* **2013**, *49*, 234–241. [CrossRef]
83. Sato, K.; Ichinose, M.; Hirotsu, Y.; Inoue, Y. Effects of deformation induced phase transformation and twinning on the mechanical properties of austenitic Fe-Mn-Al alloys. *ISIJ Int.* **1989**, *29*, 868–877. [CrossRef]
84. Bracke, L.; Mertens, G.; Penning, J.; de Cooman, B.C.; Liebeherr, M.; Akdut, N. Influence of phase transformations on the mechanical properties of high-strength austenitic Fe-Mn-Cr steel. *Metall. Mater. Trans. A* **2006**, *37*, 307–317. [CrossRef]
85. Tuluca, I.B.; Koyama, M.; Bal, B.; Canadinc, D.; Akiyama, E.; Tsuzaki, K. High-concentration carbon assists plasticity-driven hydrogen embrittlement in a Fe-high Mn steel with a relatively high stacking fault energy. *Mater. Sci. Eng. A* **2018**, *717*, 78–84. [CrossRef]
86. Fan, Y.H.; Zhang, B.; Wang, J.Q.; Han, E.H.; Ke, W. Effect of grain refinement on the hydrogen embrittlement of 304 austenitic stainless steel. *J. Mater. Sci. Technol.* **2019**, *35*, 2213–2219. [CrossRef]
87. Khedr, M.; Li, W.; Zhu, X.; Zhou, P.; Gao, S.; Jin, X. Improving hydrogen embrittlement resistance of Hadfield steel by thermo-mechanical flash-treatment. *Mater. Sci. Eng. A* **2018**, *712*, 133–139. [CrossRef]
88. Song, E.J.; Bhadeshia, H.K.D.H.; Suh, D.W. Interaction of aluminium with hydrogen in twinning-induced plasticity steel. *Scr. Mater.* **2014**, *87*, 9–12. [CrossRef]
89. Han, D.K.; Lee, S.K.; Noh, S.J.; Kim, S.K.; Suh, D.W. Effect of aluminium on hydrogen permeation of high-manganese twinning-induced plasticity steel. *Scr. Mater.* **2015**, *99*, 45–48. [CrossRef]
90. Koyama, M.; Akiyama, E.; Tsuzaki, K. Hydrogen embrittlement in Al-added twinning-induced plasticity steels evaluated by tensile tests during hydrogen charging. *ISIJ Int.* **2012**, *52*, 2283–2287. [CrossRef]
91. Park, I.J.; Jeong, K.H.; Jung, J.G.; Lee, C.S.; Lee, Y.K. The mechanism of enhanced resistance to the hydrogen delayed fracture in Al-added Fe-18Mn-0.6C twinning induced plasticity steels. *Int. J. Hydrog. Energ.* **2012**, *37*, 9925–9932. [CrossRef]
92. Koyama, M.; Okazaki, S.; Sawaguchi, T.; Tsuzaki, K. Hydrogen embrittlement susceptibility of Fe-Mn binary alloys with high Mn content: Effects of stable and metastable ε-martensite, and Mn concentration. *Metall. Mater. Trans. A* **2016**, *47*, 2656–2673. [CrossRef]
93. Lee, S.M.; Park, I.J.; Jung, J.G.; Lee, Y.K. The effect of Si on hydrogen embrittlement of Fe-18Mn-0.6C-xSi twinning induced plasticity steels. *Acta Mater.* **2016**, *103*, 264–272. [CrossRef]
94. Suzuki, S. Surface and Grain Boundary Segregation. *Corros. Eng.* **2009**, *48*, 400–404. [CrossRef]
95. García-Mazarío, M.; Lancha, A.M.; Hernández-Mayoral, M. Embrittlement susceptibility induced by impurities segregation to grain boundaries in martensitic steels candidates to be used in ADS. *J. Nucl. Mater.* **2007**, *360*, 293–303. [CrossRef]
96. Ryazanov, A. Kinetics of grain boundary fracture of irradiated materials. *Radiat. Eff. Defects Solids* **1999**, *148*, 517–533. [CrossRef]
97. Xue, K.S. *The Low Temperature Brittle Fracture of Austenitic Fe-Mn Alloys*; Lawrence Berkeley Lab.: Berkeley, CA, USA, 1986.
98. Jing, L.; Yang, H.; Ping, Y. Prolonged work hardening range in high manganese TRIP steel during adiabatic shear band formation. *Mater. Lett.* **2014**, *134*, 180–183. [CrossRef]
99. El-Sherbiny, A.; Shash, A.Y.; El-Fawkhry, M.K.; El-Hossainy, T.M.; Mattar, T. Studying the effect of manganese content on TRIP advanced high strength steel. *Mater. Sci. Forum* **2019**, *950*, 50–54. [CrossRef]
100. Li, X.; Chen, L.; Zhao, Y.; Misra, R.D.K. Influence of manganese content on ε-/α'-martensitic transformation and tensile properties of low-C high-Mn TRIP steels. *Mater. Design* **2018**, *142*, 190–202. [CrossRef]
101. Eskandari, M. Effect of deformation temperature on the mechanical behavior of a new TRIP/TWIP steel containing 21% manganese. *Int. J. ISSI* **2011**, *8*, 16–19.
102. Choi, K.; Seo, C.H.; Lee, H.; Kim, S.K.; Kwak, J.H.; Chin, K.G.; Park, K.T.; Kim, N.J. Effect of aging on the microstructure and deformation behavior of austenite base lightweight Fe-28Mn-9A1-0.8Csteel. *Scri. Mater.* **2010**, *63*, 1028–1031. [CrossRef]
103. Park, K.T.; Kim, G.; Kim, S.K.; Lee, S.W.; Hwang, S.W.; Lee, C.S. On the transitions of deformation modes of fully austenitic steels at room temperature. *Met. Mater. Int.* **2010**, *16*, 1–6. [CrossRef]
104. Gutierrez-Urrutia, I.; Raabe, D. Multistage strain hardening through dislocation substructure and twinning in a high strength and ductile weightreduced Fe-Mn-Al-C steel. *Acta Mater.* **2012**, *60*, 5791–5802. [CrossRef]

105. Razmpoosh, M.H.; Zarei-Hanzaki, A.; Haghdadi, N.; Cho, J.H.; Kim, W.J.; Heshmati-Manesh, S. Thermal stability ofan ultrafine-grained dual phase TWIP steel. *Mater. Sci. Eng. A* **2015**, *638*, 5–14. [CrossRef]
106. Gutierrez-Urrutia, I.; Raabe, D. Dislocation and twin substructure evolution during strain hardening of an Fe-22wt.%Mn-0.6wt.%C TWIP steel observed by electron channeling contrast imaging. *Acta Mater.* **2011**, *59*, 6449–6462. [CrossRef]